J. Fluid Mech. (2005), *vol.* 538, *pp.* 291–308.
doi:10.1017/S002211200500532X Printed in the United Kingdom

Unsteady hydrodynamic effect of rotation on steady rigid-body motion

By S. BHATTACHARYA

Department of Mechanical Engineering, Yale University, New Haven, CT 06520-8286, USA

(Received 1 September 2004 and in revised form 17 March 2005)

Owing to the inertial effect of the flow, an unsteady hydrodynamic force will act on a particle of arbitrary shape undergoing a steady rigid-body motion with small but finite Reynolds number if the axis of rotation of the particle is not its axis of rotational symmetry. Unsteady flow field is generated owing to such rotation of the body and as a result the particle experiences a time-dependent translational resistance. In this paper, we analyse this time-dependent hydrodynamic force and obtain its higher-order correction by systematically expanding the Navier–Stokes equation in small Reynolds number.

1. Introduction

In this paper, an arbitrary particle undergoing a steady rigid-body motion in viscous fluid is considered where the particle is rotating about an axis which is not its axis of rotational symmetry. Such rotation creates an unsteady flow near the body, even if the free-stream flow far away from the body is time independent. The inertial effect of this unsteady near field is described here for small but finite Reynolds numbers in terms of unsteady instantaneous hydrodynamic force.

In general, particle motion in creeping flow is a classical problem in hydrodynamics, and for more than a century, various effects of flow fields on the motion of particles of different shapes have been analysed. For example, the hydrodynamic resistance on a translating sphere was first studied by Stokes in 1851 and then by Basset and Oseen. More recently, such motion of a sphere was investigated in shear flow (Saffman 1965), in non-uniform flows (Mazur & Bedeaux 1974; Maxey & Riley 1983) and in oscillating flows (Mei, Lawrence & Adrian 1992; Lovalenti & Brady 1993). The effect of the rotation of a spinning sphere in a viscous fluid has also been analysed (Rubinow & Keller 1961).

For our analysis, we consider only non-spherical particles, which produce unsteady near-field because of their rotation. There are numerous studies which describe dynamics of such non-spherical particles in both steady and time-dependent free-stream flow with low Reynolds number. Such results are available for spheroids (Lawrence & Weinbaum 1986, 1988), slender bodies (Khayat & Cox 1989) and rod-like particles (Pitiman & Kasiri 1992). For arbitrary rigid bodies, the analytical expressions for force and torque have been derived with higher-order inertial corrections (Brenner & Cox 1963; Cox 1965; Chester 1990) and the flow fields around such bodies have been numerically evaluated (Youngren & Acrivos 1975). The particle dynamics was also described when the arbitrarily shaped body interacts with time-dependent flows (Gavze 1990). Similar analysis has also been published for assemblage of particles (Leshansky, Lavrenteva & Nir 2004). However, in the aforementioned

works, the unsteady near-field due to the rotation of the particle is never considered; this produces an additional time-dependent inertial correction to the hydrodynamic force on the body.

In earlier work, the effect of the rigid-body rotation on the hydrodynamic resistance was observed (Brenner 1963, 1964). However, the effect, discussed in these papers, is completely different from the inertial effect described here. In these prior papers, the flow field was considered quasi-steady and Stokesian whereas in this present work unsteadiness of the near field modifies the instantaneous hydrodynamic resistance. The problem, analysed here, has similarities with the studies of the generalized unsteady history force due to the unsteady motion of a rigid body (Lovalenti & Brady 1993, 1995). Similar physics is also observed in multi-particle systems where the time dependence of the Stokesian flow field is caused by the change in the relative position of the particles in the assemblage (Leshansky *et al.* 2004).

In order to determine the unsteady effect of particle rotation, we use Reynolds-number expansion which is presented in § 2. We derive the leading-order quantities related to zeroth-order terms in Reynolds-number expansion in § 3 and higher-order corrections in §§ 4 and 6. Examples of the effect discussed are illustrated in § 5 for linear chains and square arrays of rigidly welded spheres to demonstrate the physical implication of the analysis. Finally, conclusions are drawn in § 7.

2. Expansions of governing equations

We consider Navier–Stokes equation for non-dimensional relative velocity field ($\boldsymbol{u}$) with respect to the moving rigid body in a coordinate system translating with the particle:

$$\nabla^2\boldsymbol{u} - \nabla p = Re\left(Sl\frac{\partial \boldsymbol{u}}{\partial t} + \boldsymbol{u}\cdot\nabla\boldsymbol{u}\right), \qquad \nabla\cdot\boldsymbol{u} = 0. \tag{2.1}$$

Here, Re and Sl are the Reynolds number (UL/ν) and the Strouhal number ($L\Omega/U$) with L, U and Ω being the characteristic length, linear speed and angular speed of the body and ν denoting the kinematic viscosity. The non-dimensional position $\boldsymbol{r}$, velocity $\boldsymbol{u}$, time t and pressure p are scaled with L, U, $1/\Omega$ and $\nu U/L$. For this problem, the boundary conditions on the body surface ($\mathscr{B}$) and at the infinity are:

$$\boldsymbol{u}|_{\mathscr{B}} = Sl\ \hat{\boldsymbol{e}}_{\Omega}\times\boldsymbol{r}, \qquad \boldsymbol{u}|_{\boldsymbol{r}\to\infty} = -\hat{\boldsymbol{e}}_{u}, \tag{2.2}$$

where $\hat{\boldsymbol{e}}_u$ and $\hat{\boldsymbol{e}}_{\Omega}$ are unit vectors along the linear and the angular velocity of the body. For mathematical convenience, the origin is set on the axis of steady rotation which moves with the body in a planar locus without changing its orientation. The offset between the axis of rotation and the centre of mass of the body is considered to be of the order of L.

As the particle rotates and translates steadily, the relevant fields are periodic in time:

$$\boldsymbol{u}(\boldsymbol{r},t) = \sum_{n=-\infty}^{\infty}\boldsymbol{u}_n(\boldsymbol{r})\mathrm{e}^{\mathrm{i}nt}, \qquad p(\boldsymbol{r},t) = \sum_{n=-\infty}^{\infty}p_n(\boldsymbol{r})\mathrm{e}^{\mathrm{i}nt}. \tag{2.3}$$

Substituting (2.3) into (2.1), we find that mode velocity $\boldsymbol{u}_n$ and mode pressure p_n satisfy,

$$\nabla^2\boldsymbol{u}_n - \nabla p_n = Re\left(\mathrm{i}n\,Sl\,\boldsymbol{u}_n + \sum_{j=-\infty}^{\infty}\boldsymbol{u}_j\cdot\nabla\boldsymbol{u}_{n-j}\right), \qquad \nabla\cdot\boldsymbol{u}_n = 0. \tag{2.4}$$

In this paper, instead of (2.1), the above equations are solved for different frequency modes. We consider the Reynolds number to be less than unity and the Strouhal number to be between Re and Re^{-1} so that we can correctly apply perturbative techniques to determine the mode fields. Accordingly, we divide the domain into three subdomains (inner, intermediate and outer) and then, for the leading order, mode equations (2.4) are simplified by neglecting the corresponding inconsequential terms in each region. For higher orders, the mode velocity and pressure fields are expanded as series functions of Reynolds number. We derive hierarchical sets of equations for each term in these expansions where the neglected terms are incorporated in the next order equation in the hierarchy. Then with proper matching conditions between the fields of adjacent regions, the flow fields are solved.

2.1. *Inner expansion*

The flow field near the rigid body can be considered as viscous where the inertial terms in governing equations are negligible with respect to the viscous term. From scaling argument between the viscous and the temporal term in (2.1), it can be concluded that the mode fields should be expanded in terms of power series of $\sqrt{Re}$

$$\boldsymbol{u}_n = \sum_{m=0}^{\infty} \boldsymbol{u}_{nm} Re^{m/2}, \qquad p_n = \sum_{m=0}^{\infty} p_{nm} Re^{m/2}. \tag{2.5}$$

Substituting (2.5) into (2.4), we derive equations for the expansion velocity and pressure:

$$\nabla^2 \boldsymbol{u}_{nm} - \nabla p_{nm} = 0 \quad (m < 2), \tag{2.6a}$$

$$\nabla^2 \boldsymbol{u}_{nm} - \nabla p_{nm} = \mathrm{i} n\, Sl\, \boldsymbol{u}_{n,m-2} + \sum_{j=-\infty}^{\infty} \sum_{k=0}^{m-2} \boldsymbol{u}_{jk} \cdot \nabla \boldsymbol{u}_{n-j,m-2-k} \quad (m \geqslant 2), \tag{2.6b}$$

and

$$\nabla \cdot \boldsymbol{u}_{nm} = 0. \tag{2.6c}$$

We refer to (2.6) as inner equations.

2.2. *Intermediate and outer expansion*

The intermediate region is the region where the unsteady term in (2.1) becomes comparable to the viscous term and the convective term remains negligible. Here, the characteristic length is rescaled by $\sqrt{Re}$ and an intermediate length variable is defined:

$$\tilde{\boldsymbol{r}} = \boldsymbol{r}\sqrt{Re}. \tag{2.7}$$

Also we define intermediate mode velocity and pressure fields in the following way:

$$\tilde{\boldsymbol{u}}_n(\tilde{\boldsymbol{r}}) = \boldsymbol{u}_n(\boldsymbol{r}), \quad \tilde{p}_n(\tilde{\boldsymbol{r}}) = p_n(\boldsymbol{r})/\sqrt{Re}. \tag{2.8}$$

These intermediate fields are expanded as a polynomial series of $\sqrt{Re}$:

$$\tilde{\boldsymbol{u}}_n = \sum_{m=0}^{\infty} \tilde{\boldsymbol{u}}_{nm} Re^{m/2}, \qquad \tilde{p}_n = \sum_{m=0}^{\infty} \tilde{p}_{nm} Re^{m/2}. \tag{2.9}$$

From (2.4), we find the equation for $\tilde{\boldsymbol{u}}_{nm}$ and $\tilde{p}_{nm}$ by substituting the proper variables:

$$\tilde{\nabla}^2 \tilde{\boldsymbol{u}}_{n0} - \mathrm{i}\, n\, Sl\, \tilde{\boldsymbol{u}}_{n0} - \tilde{\nabla} \tilde{p}_{n0} = 0, \tag{2.10a}$$

$$\tilde{\nabla}^2\tilde{\boldsymbol{u}}_{nm} - \mathrm{i}\,n\,Sl\,\tilde{\boldsymbol{u}}_{nm} - \tilde{\nabla}\tilde{p}_{nm} = \sum_{j=-\infty}^{\infty}\sum_{k=0}^{m-1}\tilde{\boldsymbol{u}}_{jk}\cdot\tilde{\nabla}\tilde{\boldsymbol{u}}_{n-j,m-1-k} \quad (m \geqslant 1), \tag{2.10b}$$

and

$$\tilde{\nabla}\cdot\tilde{\boldsymbol{u}}_{nm} = 0, \tag{2.10c}$$

where, $\tilde{\nabla}$ is the gradient in $\tilde{\boldsymbol{r}}$ space. These equations are named as intermediate equations.

The flow fields in the inner and intermediate regions are the most important for obtaining the leading-order contribution of the unsteady effect of the particle rotation. Still, we present a brief discussion on the outer subdomain where the convective term in the momentum equation is comparable to the diffusive term. Here, the rescaled length is $\boldsymbol{r}' = \boldsymbol{r}Re$ and redefined mode velocity and mode pressure fields are $\boldsymbol{u}'_n(\boldsymbol{r}') = \boldsymbol{u}_n(\boldsymbol{r})$ and $p'_n(\boldsymbol{r}') = p_n(\boldsymbol{r})/Re$. We can express $\boldsymbol{u}'_n$ and p'_n as a series function of $\sqrt{Re}$ in an expansion similar to (2.9). However, for $n \neq 0$, when the unsteady term exists in (2.4), this expansion is meaningless and the expansion fields $\boldsymbol{u}'_{nm}$ and p'_{nm} are trivially zero for steady free-stream flow. For $n = 0$, when the unsteady term in (2.4) is absent, the equation for $\boldsymbol{u}'_{0m}$ and p'_{0m} is obtained considering steady and uniform free-stream flow

$$\nabla'^2\boldsymbol{u}'_{0m} - \nabla' p'_{0m} - \sum_{k=0}^{m-2}\boldsymbol{u}'_{0k}\cdot\nabla\boldsymbol{u}'_{0,m-k} = 0 \quad (m \geqslant 2), \tag{2.11}$$

which is the Oseen equation for $m = 2$. When $m < 2$, $\boldsymbol{u}'_{0,m}$ is derived from free-stream flow.

2.3. *Matching conditions between adjacent regions*

The necessary boundary conditions for the expansion equations (2.6), (2.10) and (2.11) for the three regions are derived from the matching conditions between the inner, intermediate and outer solutions. These matching conditions are deduced from the fact that if the expansions for these three regions are evaluated with an infinite number of terms all of them actually depict the same flow field. They are as follows:

$$\boldsymbol{u}'_{nm}|_{\boldsymbol{r}'\to 0} = \delta_{n0}\sum_{i=1}^{m}\tilde{\boldsymbol{u}}^{(-i)}_{n,m-i}(\tilde{\boldsymbol{r}})Re^{-i/2} \quad (m > 0), \tag{2.12a}$$

$$\tilde{\boldsymbol{u}}_{nm}|_{\tilde{\boldsymbol{r}}\to 0} = \sum_{i=1}^{m}\boldsymbol{u}^{(-i)}_{n,m-i}(\boldsymbol{r})Re^{-i/2} \quad (m > 0), \tag{2.12b}$$

$$\tilde{\boldsymbol{u}}_{nm}|_{\tilde{\boldsymbol{r}}\to\infty} = \sum_{i=0}^{m}\boldsymbol{u}'^{(i)}_{n,m-i}(\boldsymbol{r}')Re^{-i/2}, \tag{2.12c}$$

$$\boldsymbol{u}_{nm}|_{\boldsymbol{r}\to\infty} = \sum_{i=0}^{m}\tilde{\boldsymbol{u}}^{(i)}_{n,m-i}(\tilde{\boldsymbol{r}})Re^{-i/2}, \tag{2.12d}$$

where δ is the Kronecker delta and $\boldsymbol{v}^{(q)}(\boldsymbol{r})$ is the part of $\boldsymbol{v}(\boldsymbol{r})$ which behaves as $r^q(1 + k_q \log r)$. In our analysis, the constant k_q always remains zero. The conditions for $\boldsymbol{u}'_{n0}$ and $\tilde{\boldsymbol{u}}_{n0}$ at the origin are not given in (2.12). They are non-singular when $r \to 0$.

For the inner region, we solve (2.6) with the matching condition (2.12*d*) and boundary condition at the particle surface. The solutions for the intermediate region are obtained by solving (2.10) with matching conditions (2.12*b*) and (2.12*c*) whereas for the outer region, (2.11) and (2.12*a*) are solved along with the free-stream boundary condition at the infinity.

3. Zeroth-order solutions

The zeroth-order flow fields are the leading-order terms in Reynolds-number expansions of velocity fields defined as $\boldsymbol{u}'_{n0}$, $\tilde{\boldsymbol{u}}_{n0}$ and $\boldsymbol{u}_{n0}$. For the outer and intermediate region, $\boldsymbol{u}'_{n0}$ and $\tilde{\boldsymbol{u}}_{n0}$ are non-singular at the origin and satisfy the following conditions at infinity:

$$\sum_{n=-\infty}^{\infty} \boldsymbol{u}'_{n0}\, \mathrm{e}^{\mathrm{i}nt} = \sum_{n=-\infty}^{\infty} \tilde{\boldsymbol{u}}_{n0}\, \mathrm{e}^{\mathrm{i}nt} = -\hat{\boldsymbol{e}}_u. \tag{3.1}$$

Accordingly, analysis of the previous section implies

$$\boldsymbol{u}'_{n0} = \tilde{\boldsymbol{u}}_{n0} = -\hat{\boldsymbol{e}}_u \delta_{n0}. \tag{3.2}$$

The leading-order inner solution can be obtained by solving (2.6*a*) with appropriate boundary conditions (2.2). In order to do so, we revisit the earlier studies of Stokes flow around an arbitrary body (Brenner 1963, 1964). According to this analysis, the quasi-steady Stokes flow field ($\boldsymbol{v}$) around a rotating translating sphere is expressed as:

$$\boldsymbol{v} = -\hat{\boldsymbol{e}}_u + \boldsymbol{K}_u(\boldsymbol{r}) \cdot \hat{\boldsymbol{e}}_u + Sl\, \boldsymbol{K}_\Omega(\boldsymbol{r}) \cdot \hat{\boldsymbol{e}}_\Omega, \tag{3.3}$$

where $\boldsymbol{K}_u$ and $\boldsymbol{K}_\Omega$ are two position-dependent second-order tensors. This implies the unsteady zeroth-order inner field can be expressed as

$$\sum_{n=-\infty}^{\infty} \boldsymbol{u}_{n0}\, e^{\mathrm{i}nt} = -\hat{\boldsymbol{e}}_u + \boldsymbol{K}_u(\boldsymbol{r}, t) \cdot \hat{\boldsymbol{e}}_u + Sl\, \boldsymbol{K}_\Omega(\boldsymbol{r}, t) \cdot \hat{\boldsymbol{e}}_\Omega. \tag{3.4}$$

Here, the time dependence of $\boldsymbol{K}_u$ and $\boldsymbol{K}_\Omega$ arises owing to the change in the orientation of the rigid body rotating about an axis which is not an axis of rotational symmetry. The spatial dependence of $\boldsymbol{K}_u$ and $\boldsymbol{K}_\Omega$ is complicated and is dependent on the shape of the particle. However, if these tensorial functions are known at $t = 0$, their temporal evolution can be derived in terms of their respective initial values $\boldsymbol{K}_u^{\mathrm{i}}$ and $\boldsymbol{K}_\Omega^{\mathrm{i}}$.

The key step in this derivation of the temporal evolution is to recognize the time-invariant symmetries associated with the tensors $\boldsymbol{K}_u$ and $\boldsymbol{K}_\Omega$. Let us consider a set of inertial basis vectors which are not changing with time and another set of rotating basis vectors which are fixed with the body. As $\boldsymbol{K}_u$ and $\boldsymbol{K}_\Omega$ are dependent only on the shape and the orientation of the body, the representations of these tensors in the rotating basis at a point which is also rotating with the body are time independent. Therefore, we must deal with two different kinds of transformation in order to exploit this symmetry. First, we must consider the orthonormal transformation of the tensors from the rotating basis to the inertial basis and then we take into account the transformation describing the change in the position of the rotating observation point. A pictorial representation of these transformations is shown in figure 1 to reveal the intuitive justification behind the invariance of the tensorial fields.

We name this relation body invariance. Using this symmetry and considering that the axis of the steady rotation passes through the origin of the coordinate system, we

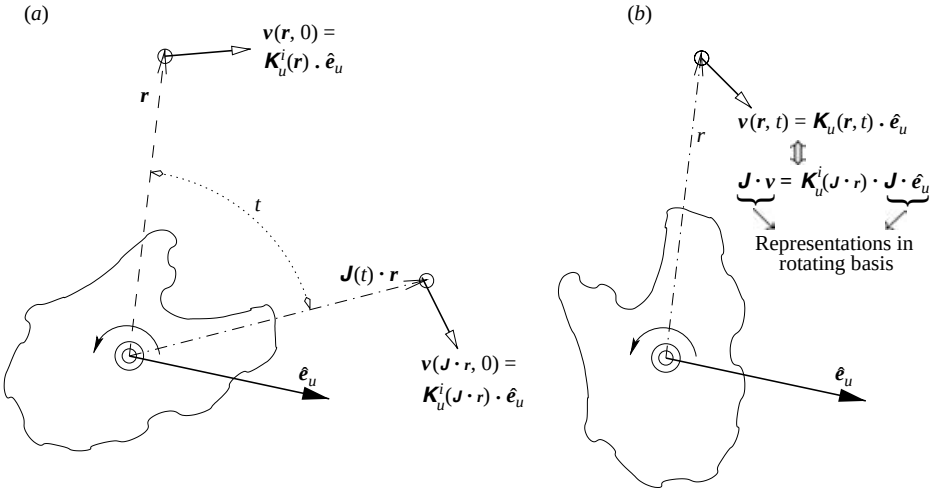

FIGURE 1. The temporal evolution of the body invariant tensor according to the symmetry relation (3.5). (*a*) The dashed vector is $\boldsymbol{r}$ at the initial time = 0. The dash-dot line indicates a vector which is rotating with the body. (*b*) When time = t, this dash-dot line coincides with $\boldsymbol{r}$. According to the body invariance symmetry, the representation of the tensor $\boldsymbol{K}_u^i$ in the rotating basis is invariant of time on the rotating dash-dot line.

find that:

$$\boldsymbol{K}_u(\boldsymbol{r},t)=\boldsymbol{J}^T(t)\cdot\boldsymbol{K}_u^{\mathrm{i}}(\boldsymbol{J}\cdot\boldsymbol{r})\cdot\boldsymbol{J}(t),\qquad \boldsymbol{K}_\Omega(\boldsymbol{r},t)=\boldsymbol{J}^T(t)\cdot\boldsymbol{K}_\Omega^{\mathrm{i}}(\boldsymbol{J}\cdot\boldsymbol{r})\cdot\boldsymbol{J}(t). \tag{3.5}$$

Here, $\boldsymbol{J}$ is the time-dependent orthonormal evolution tensor whose representation in terms of the inertial basis is the same as the orthonormal transformation matrix between the rotating and the inertial basis. Hence,

$$\boldsymbol{J}(t)=(\boldsymbol{I}-\hat{\boldsymbol{e}}_\Omega\hat{\boldsymbol{e}}_\Omega)\cos t+\hat{\boldsymbol{e}}_\Omega\hat{\boldsymbol{e}}_\Omega+\boldsymbol{E}\cdot\hat{\boldsymbol{e}}_\Omega\sin t, \tag{3.6}$$

where $\boldsymbol{I}$ and $\boldsymbol{E}$ are the second-order identity tensor and the third-order permutation tensor.

Tensors $\boldsymbol{K}_u^{\mathrm{i}}$ and $\boldsymbol{K}_\Omega^{\mathrm{i}}$ are singular at the origin and decay at infinity as a summation of decaying tensorial terms with different negative powers of distance r. Among them, the tensors $\boldsymbol{K}_{u(-1)}^{\mathrm{i}}$ and $\boldsymbol{K}_{\Omega(-1)}^{\mathrm{i}}$, which decay as the inverse of the distance from the origin, are of special interest for two reasons. First, they are associated with $\boldsymbol{u}_{n0}^{(-1)}$ which provides the matching condition for the next higher-order equation for the intermediate subdomain in (2.12*b*). Secondly, they are required in order to evaluate the zeroth-order hydrodynamic force on the particle. These two tensors which decay as $1/r$ at infinity are:

$$\boldsymbol{K}_{u(-1)}^{\mathrm{i}}(\boldsymbol{J}\cdot\boldsymbol{r})=\boldsymbol{T}(\boldsymbol{J}\cdot\boldsymbol{r})\cdot\boldsymbol{F}_{\mathrm{i}},\qquad \boldsymbol{K}_{\Omega(-1)}^{\mathrm{i}}(\boldsymbol{J}\cdot\boldsymbol{r})=\boldsymbol{T}(\boldsymbol{J}\cdot\boldsymbol{r})\cdot\bar{\boldsymbol{F}}_{\mathrm{i}}, \tag{3.7}$$

where the origin is on the axis of steady rotation and $\boldsymbol{T}$ is the Oseen tensor

$$\boldsymbol{T}(\boldsymbol{r})=\frac{1}{8\pi}\left(\frac{\boldsymbol{I}}{r}+\frac{\boldsymbol{r}\boldsymbol{r}}{r^3}\right). \tag{3.8}$$

Constant tensors, represented as $\boldsymbol{F}_{\mathrm{i}}$ and $\bar{\boldsymbol{F}}_{\mathrm{i}}$, are translation–translation and translation–rotation friction tensors and are known for specific shape and initial orientation of the particle. Subscript i indicates that these tensors are determined at the initial time.

From the definition of $\boldsymbol{u}_{n0}^{(-1)}$ in § 2.3 and (3.4), (3.5) and (3.7), the zeroth-order inner flow field decaying as $1/r$ can be expressed as

$$\sum_{n=-\infty}^{\infty} \boldsymbol{u}_{n0}^{(-1)} \mathrm{e}^{\mathrm{i}nt} = \boldsymbol{J}^T(t)\cdot\boldsymbol{T}(\boldsymbol{J}\cdot\boldsymbol{r})\cdot\boldsymbol{F}_{\mathrm{i}}\cdot\boldsymbol{J}(t)\cdot\hat{\boldsymbol{e}}_u + Sl\,\boldsymbol{J}^T(t)\cdot\boldsymbol{T}(\boldsymbol{J}\cdot\boldsymbol{r})\cdot\bar{\boldsymbol{F}}_{\mathrm{i}}\cdot\boldsymbol{J}(t)\cdot\hat{\boldsymbol{e}}_\Omega. \tag{3.9}$$

Substituting (3.6) and (3.8) into (3.9) and replacing $\cos t$ and $\sin t$ in the expression of $\boldsymbol{J}$ by $\mathrm{e}^{\mathrm{i}t}$ and $\mathrm{e}^{-\mathrm{i}t}$, we derive the explicit expressions for $\boldsymbol{u}_{n0}^{(-1)}$

$$\boldsymbol{u}_{n0}^{(-1)} = \boldsymbol{T}(\boldsymbol{r})\cdot\boldsymbol{f}_{n0}. \tag{3.10}$$

Here, $\boldsymbol{f}_{n0}$ is the amplitude of the non-dimensional force oscillating in time with $n/2\pi$ frequency:

$$\boldsymbol{f}_{0,0} = \left[\boldsymbol{J}_1^T\cdot\boldsymbol{F}_{\mathrm{i}}\cdot\boldsymbol{J}_{-1} + \boldsymbol{J}_0^T\cdot\boldsymbol{F}_{\mathrm{i}}\cdot\boldsymbol{J}_0 + \boldsymbol{J}_{-1}^T\cdot\boldsymbol{F}_{\mathrm{i}}\cdot\boldsymbol{J}_1\right]\cdot\hat{\boldsymbol{e}}_u + Sl\,\boldsymbol{J}_0^T\cdot\bar{\boldsymbol{F}}_{\mathrm{i}}\cdot\hat{\boldsymbol{e}}_\Omega, \tag{3.11a}$$

$$\boldsymbol{f}_{1,0} = \boldsymbol{f}_{-1,0}^{*} = \left[\boldsymbol{J}_1^T\cdot\boldsymbol{F}_{\mathrm{i}}\cdot\boldsymbol{J}_0 + \boldsymbol{J}_0^T\cdot\boldsymbol{F}_{\mathrm{i}}\cdot\boldsymbol{J}_1\right]\cdot\hat{\boldsymbol{e}}_u + Sl\,\boldsymbol{J}_1^T\cdot\bar{\boldsymbol{F}}_{\mathrm{i}}\cdot\hat{\boldsymbol{e}}_\Omega, \tag{3.11b}$$

$$\boldsymbol{f}_{2,0} = \boldsymbol{f}_{-2,0}^{*} = \boldsymbol{J}_1^T\cdot\boldsymbol{F}_{\mathrm{i}}\cdot\boldsymbol{J}_1\cdot\hat{\boldsymbol{e}}_u, \tag{3.11c}$$

where $*$ indicates complex conjugate. The tensors $\boldsymbol{J}_0$, $\boldsymbol{J}_1$ and $\boldsymbol{J}_{-1}$ are obtained from the expansion $\boldsymbol{J}(t) = \sum_{n=-1}^{1}\boldsymbol{J}_n\mathrm{e}^{\mathrm{i}nt}$:

$$\boldsymbol{J}_0 = \hat{\boldsymbol{e}}_\Omega\hat{\boldsymbol{e}}_\Omega, \qquad \boldsymbol{J}_1 = (\boldsymbol{I} - \hat{\boldsymbol{e}}_\Omega\hat{\boldsymbol{e}}_\Omega - \mathrm{i}\boldsymbol{E}\cdot\hat{\boldsymbol{e}}_\Omega)/2, \qquad \boldsymbol{J}_{-1} = \boldsymbol{J}_1^T = \boldsymbol{J}_1^{*}. \tag{3.12}$$

When $|n| > 2$, $\boldsymbol{f}_{n0}$ is zero. Therefore, net zeroth-order force on the rigid body is

$$\boldsymbol{f}_0 = \eta U L\sum_{n=-2}^{2}\boldsymbol{f}_{n0}\,\mathrm{e}^{\mathrm{i}nt}. \tag{3.13}$$

This equation along with (3.11) and (3.12) describes the unsteady zeroth-order force on the rotating–translating particle and (3.10) is used to obtain first-order inertial correction.

The time average of the leading-order force is an important quantity because it governs the dynamics of the particle in large time scale. The zeroth-order time-averaged force is represented by $\boldsymbol{f}_{0,0}$, and from (3.11*a*) we present its detailed structure:

$$\langle\boldsymbol{f}_0\rangle = \eta U L\,\boldsymbol{f}_{0,0} = \eta U L\left[\frac{1}{2}\tau(\boldsymbol{I} - \hat{\boldsymbol{e}}_\Omega\hat{\boldsymbol{e}}_\Omega) + \tau_2\hat{\boldsymbol{e}}_\Omega\hat{\boldsymbol{e}}_\Omega\right]\cdot\hat{\boldsymbol{e}}_u + (\hat{\boldsymbol{e}}_\Omega\cdot\bar{\boldsymbol{F}}_{\mathrm{i}}\cdot\hat{\boldsymbol{e}}_\Omega)\hat{\boldsymbol{e}}_\Omega. \tag{3.14}$$

Here, τ_1 is the trace of the tensor $(\boldsymbol{I} - \hat{\boldsymbol{e}}_\Omega\hat{\boldsymbol{e}}_\Omega)\cdot\boldsymbol{F}_{\mathrm{i}}$, whereas τ_2 is $\hat{\boldsymbol{e}}_\Omega\cdot\boldsymbol{F}_{\mathrm{i}}\cdot\hat{\boldsymbol{e}}_\Omega$.

The unsteady component of the Stokesian force in (3.13) is zero when an axisymmetric body rotates around its axis of rotational symmetry. For such cases, in (3.11), the tensors $\boldsymbol{F}_{\mathrm{i}}$ and $\boldsymbol{J}_j$ commute:

$$\boldsymbol{J}_j^T\cdot\boldsymbol{F}_{\mathrm{i}} = \boldsymbol{F}_{\mathrm{i}}\cdot\boldsymbol{J}_j^T \quad \boldsymbol{J}_j^T\cdot\bar{\boldsymbol{F}}_{\mathrm{i}} = \bar{\boldsymbol{F}}_{\mathrm{i}}\cdot\boldsymbol{J}_j^T \qquad (j = 0, \pm 1). \tag{3.15}$$

Owing to this commuting property, for axisymmetric rotation, the expressions for the vibrating modes in (3.13) involve products such as $\boldsymbol{J}_0^T\cdot\boldsymbol{J}_{\pm1}$, $\boldsymbol{J}_1^T\cdot\boldsymbol{J}_1$, $\boldsymbol{J}_{-1}^T\cdot\boldsymbol{J}_{-1}$ and $\boldsymbol{J}_{\pm1}^T\cdot\hat{\boldsymbol{e}}_\Omega$ which are identically zero. Thus, such rotation cannot create any unsteady force. Also, we can consider another special case where the linear velocity of the body is co-linear to its angular velocity. Then the force which vibrates with frequency $1/\pi$ is zero because then $\boldsymbol{J}_{\pm1}\cdot\hat{\boldsymbol{e}}_u = 0$.

For the higher-order inertial correction, the matching condition (2.12) requires an expression for $\boldsymbol{u}_{n0}^{(-2)}$ which decays as r^{-2} at infinity. We follow the same procedure

to derive $\boldsymbol{u}_{n0}^{(-2)}$ as we did for $\boldsymbol{u}_{n0}^{(-1)}$ by defining tensors $\boldsymbol{K}^{\mathrm{i}}_{u(-2)}$ and $\boldsymbol{K}^{\mathrm{i}}_{\Omega(-2)}$ which are inversely proportional to the square of distance r:

$$\sum_n \boldsymbol{u}_{n0}^{(-2)}\,\mathrm{e}^{\mathrm{i}nt} = \boldsymbol{J}^T(t)\cdot\boldsymbol{K}^{\mathrm{i}}_{u(-2)}(\boldsymbol{J}\cdot\boldsymbol{r})\cdot\boldsymbol{J}(t)\cdot\hat{\boldsymbol{e}}_u + Sl\,\boldsymbol{J}^T(t)\cdot\boldsymbol{K}^{\mathrm{i}}_{\Omega(-2)}(\boldsymbol{J}\cdot\boldsymbol{r})\cdot\boldsymbol{J}(t)\cdot\hat{\boldsymbol{e}}_\Omega, \tag{3.16}$$

where,

$$\boldsymbol{K}^{\mathrm{i}}_{u(-2)}(\boldsymbol{J}\cdot\boldsymbol{r}) = \boldsymbol{S}(\boldsymbol{J}\cdot\boldsymbol{r}):\boldsymbol{G}_{\mathrm{i}}, \qquad \boldsymbol{K}^{\mathrm{i}}_{\Omega(-2)}(\boldsymbol{J}\cdot\boldsymbol{r}) = \boldsymbol{S}(\boldsymbol{J}\cdot\boldsymbol{r}):\bar{\boldsymbol{G}}_{\mathrm{i}}. \tag{3.17}$$

In component form, the third-order tensor $\boldsymbol{S}$ is

$$S^{ijk}(\boldsymbol{r}) = \hat{\boldsymbol{e}}_j\cdot\nabla\boldsymbol{T}:\hat{\boldsymbol{e}}_i\hat{\boldsymbol{e}}_k = \frac{1}{8\pi r^3}\left(\delta_{ij}r_k + r_i\delta_{jk} - r_j\delta_{ik} - \frac{3r_ir_jr_k}{r^2}\right), \tag{3.18}$$

whereas $\boldsymbol{G}_{\mathrm{i}}$ and $\bar{\boldsymbol{G}}_{\mathrm{i}}$ are two constant third-order tensors which can be determined for specific shape and initial orientation of the particle. They satisfy the following condition

$$G^{iij}_{\mathrm{i}} = \bar{G}^{iij}_{\mathrm{i}} = 0. \tag{3.19}$$

By using (3.16)–(3.18), we obtained $\boldsymbol{u}_{n0}^{(-2)}$,

$$\boldsymbol{u}_{n0}^{(-2)} = \boldsymbol{S}(\boldsymbol{r}):\boldsymbol{g}_{n0}. \tag{3.20}$$

The second-order tensor $\boldsymbol{g}_{n0}$ is zero for $|n|>3$. For $0\leqslant n\leqslant 3$, components of $\boldsymbol{g}_{n0}$ are:

$$g^{ij}_{n0} = g^{*ij}_{-n0} = \sum_{p=p'(n)}^{1}\sum_{q=q'(n,p)}^{q''(n,p)} J_p^{\lambda i}J_q^{\mu j}J_{n-p-q}^{\nu k}G^{\lambda\mu\nu}_{\mathrm{i}}e^k_u + a_n\,Sl\sum_{p=n-1}^{1}J_p^{\lambda i}J_{n-p}^{\mu j}\bar{G}^{\lambda\mu k}_{\mathrm{i}}e^k_\Omega, \tag{3.21}$$

where $p'(n)=Max(-1,n-2)$, $q'(n,p)=Max(-1,n-p-1)$, $q''(n,p)=Min(1,n-p+1)$ and $a_n=1-\delta_{n3}$. *Max* and *Min* take greater and smaller values between the arguments.

4. First-order inertial correction

The first-order inertial correction to the hydrodynamic resistance on the particle depends on the first-order velocity fields $\boldsymbol{u}'_{n1}$, $\tilde{\boldsymbol{u}}_{n1}$ and $\boldsymbol{u}_{n1}$, of which the outer velocity field $\boldsymbol{u}'_{n1}$ is trivially zero. This is concluded from the governing equation (2.11), the matching condition (2.12*a*) and the boundary condition at infinity imposed by the free-stream flow. Hence, in order to determine the first-order correction, we focus only on derivation of the first-order intermediate field $\tilde{\boldsymbol{u}}_{n1}$ and inner field $\boldsymbol{u}_{n1}$.

4.1. *Intermediate flow field*

For the first-order intermediate flow field $\tilde{\boldsymbol{u}}_{n1}$, the governing equation is described by (2.10*b*) and (2.10*c*). Considering $\tilde{\boldsymbol{u}}_{n0}=-\hat{\boldsymbol{e}}_u\delta_{n0}$ as a constant field according to (3.2), we transform (2.10*b*) into the following form for $m=1$:

$$\tilde{\nabla}^2\tilde{\boldsymbol{u}}_{n1} - \mathrm{i}n\,Sl\,\tilde{\boldsymbol{u}}_{n1} - \tilde{\nabla}\tilde{p}_{n1} = 0. \tag{4.1}$$

Also according to the matching conditions (2.12*b*) and (2.12*c*), $\tilde{\boldsymbol{u}}_{n1}$ satisfies the following boundary conditions

$$\tilde{\boldsymbol{u}}_{n1}|_{\tilde{\boldsymbol{r}}\to 0} = \frac{1}{\sqrt{Re}}\boldsymbol{T}(\boldsymbol{r})\cdot\boldsymbol{f}_{n0} = \boldsymbol{T}(\tilde{\boldsymbol{r}})\cdot\boldsymbol{f}_{n0}, \qquad \tilde{\boldsymbol{u}}_{n1}|_{\tilde{\boldsymbol{r}}\to\infty} = 0. \tag{4.2}$$

The above boundary conditions are obtained by using zeroth-order results (3.10) and (3.2) in matching conditions (2.12*b*) and (2.12*c*).

Solution for $\tilde{\boldsymbol{u}}_{n1}$ can be derived analytically:

$$\tilde{\boldsymbol{u}}_{n1} = \tilde{\boldsymbol{T}}_n(\tilde{\boldsymbol{r}}) \cdot \boldsymbol{f}_{n0}, \tag{4.3}$$

where the second-order tensor $\tilde{\boldsymbol{T}}_n$ is

$$\tilde{\boldsymbol{T}}_n(\tilde{\boldsymbol{r}}) = \frac{1}{8\pi\tilde{r}}\left[\boldsymbol{I}\,\phi_n(\tilde{r}) + \frac{\tilde{\boldsymbol{r}}\tilde{\boldsymbol{r}}}{\tilde{r}^2}\,\psi_n(\tilde{r})\right]. \tag{4.4}$$

The scalar functions ϕ_n and ψ_n are equal to 1 for $n = 0$. Otherwise,

$$\phi_n(\tilde{r}) = \frac{2\mathrm{i}}{n\,Sl\,\tilde{r}^2}\left[1 - \mathrm{e}^{-c_n\tilde{r}}\left(c_n^2\tilde{r}^2 + c_n\tilde{r} + 1\right)\right] \quad (n \neq 0), \tag{4.5}$$

and

$$\psi_n(\tilde{r}) = \frac{2\mathrm{i}}{n\,Sl\,\tilde{r}^2}\left[\mathrm{e}^{-c_n\tilde{r}}\left(c_n^2\tilde{r}^2 + 3c_n\tilde{r} + 3\right) - 3\right] \quad (n \neq 0), \tag{4.6}$$

where

$$c_n = \sqrt{|n|\,Sl}\,\mathrm{e}^{\mathrm{i}\pi|n|/4n}. \tag{4.7}$$

The real part of c_n is always positive so that $\tilde{\boldsymbol{u}}_{n1}$ decays at infinity.

The solutions for the inner region for $m = 1, 2$ depend on $\tilde{\boldsymbol{u}}_{n1}^{(0)}$ and $\tilde{\boldsymbol{u}}_{n1}^{(1)}$ because they provide the necessary boundary conditions for $\boldsymbol{u}_{n1}$ and $\boldsymbol{u}_{n2}$ through the matching condition (2.12*d*). Therefore we derive the expressions for $\tilde{\boldsymbol{u}}_{n1}^{(0)}$ and $\tilde{\boldsymbol{u}}_{n1}^{(1)}$ from $\tilde{\boldsymbol{u}}_{n1}$

$$\tilde{\boldsymbol{u}}_{n1}^{(0)} = -\frac{c_n}{6\pi}\boldsymbol{f}_{n0}, \qquad \tilde{\boldsymbol{u}}_{n1}^{(1)} = \frac{\mathrm{i}\,n\,Sl\,\tilde{r}}{32\pi}(3\boldsymbol{I} - \tilde{\boldsymbol{r}}\tilde{\boldsymbol{r}}/\tilde{r}^2)\cdot\boldsymbol{f}_{n0} \tag{4.8}$$

and use them in the analysis of inner region.

4.2. *Inner flow field*

We solve (2.6*a*) and (2.6*c*) with boundary condition (2.2) and (2.12*d*) to obtain $\boldsymbol{u}_{n1}$. The matching condition (2.12*d*) and expression for $\tilde{\boldsymbol{u}}_{n1}^{(0)}$ (4.8) imply

$$\boldsymbol{u}_{n1}|_{\boldsymbol{r}\to\infty} = -\frac{c_n}{6\pi}\boldsymbol{f}_{n0}. \tag{4.9}$$

The derivation of $\boldsymbol{u}_{n1}$ is similar to that of $\boldsymbol{u}_{n0}$

$$\sum_{n=-\infty}^{\infty}\boldsymbol{u}_{n1}\,\mathrm{e}^{\mathrm{i}nt} = \sum_{n'=-2}^{2}\frac{c_{n'}}{6\pi}\mathrm{e}^{\mathrm{i}n't}[-\boldsymbol{f}_{n'0} + \boldsymbol{K}_u(\boldsymbol{r}, t)\cdot\boldsymbol{f}_{n'0}]. \tag{4.10}$$

As for the zeroth order, here also we concentrate on deriving $\boldsymbol{u}_{n1}^{(-1)}$ which decays as $1/r$

$$\sum_{n=-\infty}^{\infty}\boldsymbol{u}_{n1}^{(-1)}\,\mathrm{e}^{\mathrm{i}nt} = \sum_{n'=-2}^{2}\frac{c_{n'}}{6\pi}\mathrm{e}^{\mathrm{i}n't}\boldsymbol{J}^T(t)\cdot\boldsymbol{T}(\boldsymbol{J}\cdot\boldsymbol{r})\cdot\boldsymbol{F}_{\mathrm{i}}\cdot\boldsymbol{J}(t)\cdot\boldsymbol{f}_{n'0}. \tag{4.11}$$

From the above equation, the expression for $\boldsymbol{u}_{n1}^{(-1)}$ is obtained in the same way for $\boldsymbol{u}_{n0}^{(-1)}$

$$\boldsymbol{u}_{n1}^{(-1)} = \boldsymbol{T}(\boldsymbol{r})\cdot\boldsymbol{f}_{n1}. \tag{4.12}$$

The first-order non-dimensional force $\boldsymbol{f}_{n1}$, with $n/2\pi$ oscillation frequency, is

$$\boldsymbol{f}_{n1} = \sum_{i=-2}^{2}\frac{c_i}{6\pi}\boldsymbol{M}_{n-i}\cdot\boldsymbol{f}_{i0} \tag{4.13}$$

where second-order tensors $\boldsymbol{M}_n$ are zero for $|n| > 2$ and otherwise they are

$$\boldsymbol{M}_0 = \boldsymbol{J}_1^T \cdot \boldsymbol{F}_\mathrm{i} \cdot \boldsymbol{J}_{-1} + \boldsymbol{J}_0^T \cdot \boldsymbol{F}_\mathrm{i} \cdot \boldsymbol{J}_0 + \boldsymbol{J}_{-1}^T \cdot \boldsymbol{F}_\mathrm{i} \cdot \boldsymbol{J}_1, \tag{4.14a}$$

$$\boldsymbol{M}_1 = \boldsymbol{M}_{-1}^* = \boldsymbol{J}_1^T \cdot \boldsymbol{F}_\mathrm{i} \cdot \boldsymbol{J}_0 + \boldsymbol{J}_0^T \cdot \boldsymbol{F}_\mathrm{i} \cdot \boldsymbol{J}_1, \tag{4.14b}$$

$$\boldsymbol{M}_2 = \boldsymbol{M}_{-2}^* = \boldsymbol{J}_1^T \cdot \boldsymbol{F}_\mathrm{i} \cdot \boldsymbol{J}_1. \tag{4.14c}$$

These tensors can be determined from the expressions of $\boldsymbol{J}_0$, $\boldsymbol{J}_1$ and $\boldsymbol{J}_{-1}$ in (3.12).

The first-order correction to the hydrodynamic force on the body can be written as a summation of force-harmonics. When (4.13) and (4.14) are considered, it seems that the frequency of vibrating force varies from -4 to 4. However, careful analysis shows, $f_{3,1} = f_{-3,1} = f_{4,1} = f_{-4,1} = 0$ because of the structure of $\boldsymbol{f}_{n0}$ in (3.11). Therefore,

$$\boldsymbol{f}_1 = \eta U L \sqrt{Re} \sum_{n=-2}^{2} \boldsymbol{f}_{n1} \, \mathrm{e}^{\mathrm{i}nt}, \tag{4.15}$$

where $\boldsymbol{f}_1$ is the first-order inertial correction to the unsteady hydrodynamic force.

5. Hydrodynamic effect of rotation on clusters of spheres

In this section, the effect of the first-order inertial correction to the hydrodynamic force on a rotating object is demonstrated by considering steady rotation and translation of clusters of rigidly attached spheres of radius a. The clusters are either linear chains of connected spheres or square grids of spheres welded in a plane. The first type of cluster represents rod-like slender bodies, whereas the second kind can be a model of plate-like objects. The number of spheres either in the linear chains or along one side of the square grids is denoted by N. Here, for both the chains and the square grids, two cases are considered with $N = 2, 8$.

For this problem, the characteristic length scale is of the order of the length of the chains or of the width of the arrays. Therefore, we set $L = aN$ and the Reynolds number and the Strouhal number are determined accordingly. For the first-order corrective force, results are presented in the rescaled form $\bar{\boldsymbol{f}}_1 = \boldsymbol{f}_1 / \sqrt{ReSl}$.

At the initial instant, we consider the linear chains to be along the x-axis and the square grids to be on the (x, z)-plane where the sides of the squares are parallel to the x- or z-axis. The objects are rotating about the z-axis and the centre of this steady rotation is at the midsection of the object. For such rotation, the vertical translation of the chain along the z-axis does not produce significant unsteadiness owing the geometrical symmetry. However, when the cluster moves in the horizontal plane, we can observe a substantial unsteady effect of the rotation. We choose the translation of the chain in the x-direction. It is to be noted that this choice does not reduce the generality of the physics described because any other choice of translation would only contribute in a temporal phase difference in the dynamical solution.

The Stokes resistant matrices of the linear chains have been calculated by (Bhattacharya, Blawzdziewicz & Wajnryb 2005). Similar results can be obtained for the square grids also. In both cases, the representation of the translation–translation friction $\boldsymbol{F}_\mathrm{i}$ in the basis vectors along x, y and z coordinates is diagonal for the initial orientation. These diagonal elements are normalized by the corresponding values for a sphere of radius L and are given in table 1. As the centre of rotation is at the middle of the array, $\bar{\boldsymbol{F}}_\mathrm{i} = \boldsymbol{0}$.

In figure 2, the normalized horizontal components of the instantaneous zeroth-order viscous force and first-order corrective force are plotted as a function of time.

	$F_i^{xx}/6\pi N$	$F_i^{yy}/6\pi N$	$F_i^{zz}/6\pi N$
Linear chain $N=2$	0.645	0.725	0.725
Linear chain $N=8$	0.322	0.435	0.435
Square grid $N=2$	0.888	0.997	0.888
Square grid $N=8$	0.747	0.986	0.747

TABLE 1. The ratio between the translation–translation friction elements for the objects in their initial orientation and the same for a sphere of radius $L = aN$. The objects are either rigid linear chains of spheres aligned along the x-axis or square arrays of rigidly attached sphere in the (x, z)-plane. The number of spheres either in the linear chain or along one side of the square array is N.

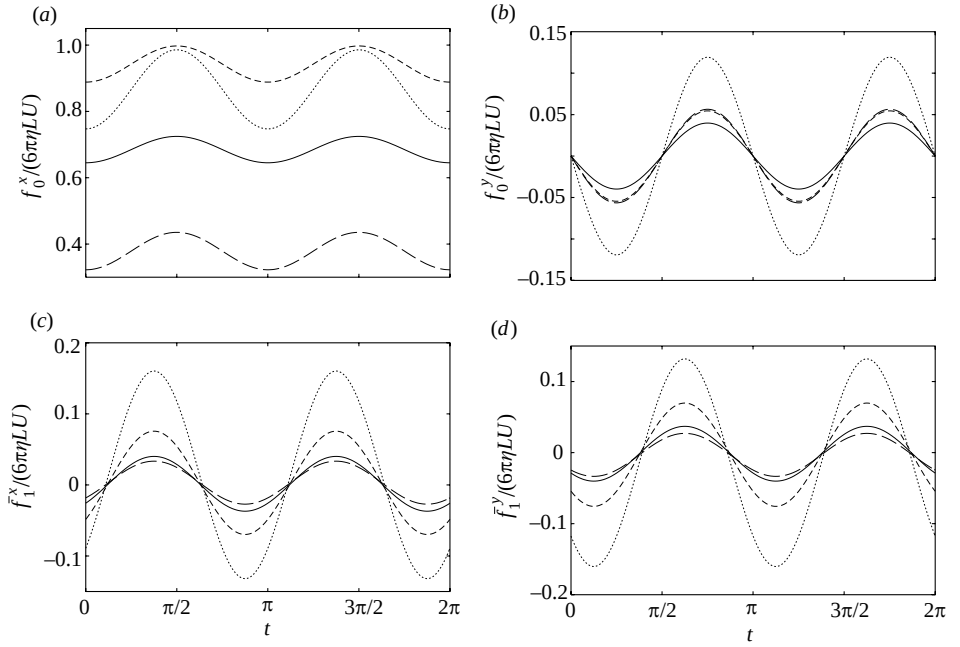

FIGURE 2. Normalized zeroth-order and first-order instantaneous hydrodynamic force on the body as a function of time. The plots present components of the horizontal forces for one-dimensional chains of welded spheres with $N = 2$ (solid line) and $N = 8$ (long dash line), and for square grids of welded spheres in a two-dimensional plane with the number of particles along one side of the square being $N = 2$ (short dash line) and $N = 8$ (dotted line).

The time period is such that the object will go through a full rotation in this interval. The curves show that these forces are sinusoidal functions of time with frequency $1/\pi$ superposed on a steady constant. For a general object, there might be another vibrating mode with frequency $1/2\pi$. However, if the direction of the angular velocity coincides with the direction of one of the eigenvectors of the Stokes resistance tensor, there will be no oscillatory force with frequency $1/2\pi$.

The amplitudes of the sinusoidal curves for the zeroth-order force depend on the difference in the magnitude of two eigenvalues of the Stokes resistance matrix in the horizontal plane (table 1). This difference is more for plate-like bodies than for linear objects and increases with N. This is why the amplitude of oscillation is largest for the square grids with $N = 8$ and least for the linear chain with $N = 2$. The mean

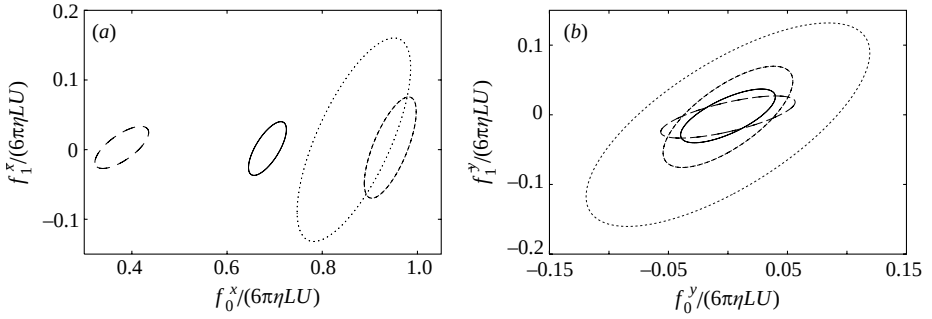

FIGURE 3. Phase diagram of the zeroth-order viscous force and the first-order inertial correction presenting the values of both forces at a particular time which varies as a parameter in the plots. (*a*) x components; (*b*) y components. The line types are as in figure 2.

value of the zeroth-order force, on the other hand, depends on the summation of the eigenvalues of the horizontal eigenvectors. Accordingly, among the objects considered, this mean value is maximum for the square grid with $N = 2$ and is minimum for the linear chain with $N = 8$. This observation is consistent with the values in table 1. The time-averaged Stokesian force on the rotating body always acts in the opposite direction of the translation of the particle which is manifested in the f_0^y–t plots where the curves oscillate about zero.

The amplitude of the oscillatory part of the first-order correction is proportional to the difference between the square of the horizontal eigenvalues and is of similar nature as that of the zeroth-order force. Unlike the zeroth-order force, the average value of the first-order force acts at an angle of $3\pi/4$ with respect to the direction of the translational velocity when the body rotates counterclockwise. If the direction of rotation is reversed, the lift component of this average force reverses its direction while the drag component remains unchanged. This line of action is independent of the shape of the body as long as the angular velocity vector is an eigenvector of $\boldsymbol{F}_{\mathrm{i}}$. The magnitude of the mean first-order force is proportional to the square of the differences in the relevant eigenvalues and it increases substantially with N, especially for the square grids.

The figures reveal that there are phase differences between f_0^x, f_0^y, f_1^x and f_1^y. The first-order correction leads the zeroth-order force by a temporal phase of $\pi/8$. On the other hand, the y-components of the force lag with respect to the corresponding x-components by $\pi/4$. These temporal phase differences are shape independent. This is why, in each subplot of figure 2, the curves for different objects show no phase difference between them.

In figure 3, the effect of the phase difference is revealed. In these plots, the instantaneous values of the zeroth- and the first-order forces are represented by a point whereas time varies along the curve as a parameter. The plots are Lissajous figures which illustrate the mean values, amplitudes and phase difference between two quantities. The earlier observations on the average and the amplitude of the zeroth- and first-order force are corroborated by this figure.

The oblique ellipses appear in the plots because of the phase difference of $\pi/8$; (phase difference of $\pm\pi/2$ would have produced straight lines with slope ±1 whereas $\pm\pi/4$ would generate a straight ellipse). This is a well-known fact about the Lissajous figures when the frequency of vibration is $1/\pi$. In general, for an arbitrary body, where the forces also oscillate with a frequency of $1/2\pi$ along with $1/\pi$, a f_1–f_0 phase

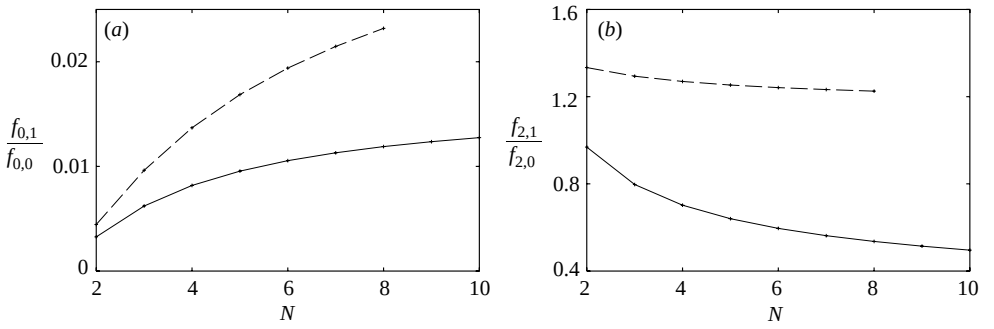

FIGURE 4. (*a*) The ratio between the magnitude of the steady part of the first-order inertial correction and the same of the zeroth-order viscous force. (*b*) The ratio between the amplitude of the vibrating part of the first-order inertial correction and the same of the zeroth-order viscous force. Both ratios are obtained for the one-dimensional chains of welded spheres (solid line) and the square grids of welded spheres in a two-dimensional plane (dashed line). The ratios are plotted as a function of the number of spheres N either in the chains or along one side of the square.

plot will be a more complicated Lissajous curve than a simple ellipse. However, in spite of its simplicity, the present plot reveals all the essential physics.

The previous discussion indicates that the geometrical effect of the shape of the body affects the amplitudes of the sinusoidal oscillation and the mean values of the forces through the horizontal eigenvalues of the Stokes resistance. These eigenvalues depend on the number N. Therefore, in figure 4, we have studied the effect of N on the hydrodynamic forces. The ratio between the averages of the first-order force and the Stokesian force are plotted along with the ratio of their oscillatory amplitudes as a function of N to understand the relative importance of the inertial correction.

The mean value of the first-order force increases with N, whereas the time-averaged zeroth-order force decreases for larger N. As a result, the ratio between them increases with the number of particles, especially for the square grids. In contrast, the ratio of the two amplitudes has a decreasing trend because this ratio is proportional to $F_{\mathrm{i}}^{xx} + F_{\mathrm{i}}^{yy}$ which is less for larger N. With increasing N, the summation diminishes faster for the linear chains. This is why the ratio between the amplitudes for the chains has a faster decay for higher values of N.

6. Second-order inertial correction

In this section, we determine the second-order inertial correction to the hydrodynamic resistance in order to illustrate how the matching condition in (2.12) can be used to avoid the Whitehead paradox in such problems. For this purpose, we derived the second-order fields $\boldsymbol{u}'_{n2}$, $\tilde{\boldsymbol{u}}_{n2}$ and $\boldsymbol{u}_{n2}$ to obtain this $O(Re)$ correction to the hydrodynamic resistance.

6.1. *Second-order outer solution*

The second-order outer velocity field is trivially zero for $n \neq 0$. When $n = 0$, the outer flow field $\boldsymbol{u}'_{0,2}$, is governed by the Oseen equation which can be obtained from (2.11) and (3.2),

$$\nabla'^2 \boldsymbol{u}'_{0,2} + \hat{\boldsymbol{e}}_u \cdot \nabla \boldsymbol{u}'_{0,2} - \nabla' p'_{0,2} = 0. \tag{6.1}$$

At infinity, $\boldsymbol{u}'_{0,2}$ decays to zero and at the origin, according to matching condition (2.12*a*),

$$\boldsymbol{u}'_{0,2}|_{r'\to 0} = \tilde{\boldsymbol{u}}^{(-1)}_{0,1}(\tilde{\boldsymbol{r}})Re^{-1/2} + \tilde{\boldsymbol{u}}^{(-2)}_{0,0}(\tilde{\boldsymbol{r}})Re^{-1} = \tilde{\boldsymbol{T}}_0(\tilde{\boldsymbol{r}})\cdot \boldsymbol{f}_{0,0}\, Re^{-1/2} = \boldsymbol{T}(\boldsymbol{r}')\cdot \boldsymbol{f}_{0,0}. \tag{6.2}$$

The solution of (6.1) and (6.2) is known (Brenner & Cox 1963). Here, instead of $\boldsymbol{u}_{0,2}$, we only describe $\boldsymbol{u}^{(0)}_{0,2}$ which provides the necessary matching condition (2.12*c*) for $\tilde{\boldsymbol{u}}_{02}$.

$$\boldsymbol{u}^{(0)}_{0,2} = \frac{1}{32\pi}[\hat{\boldsymbol{e}}_u\cdot\nabla'(\boldsymbol{r}'\boldsymbol{r}'\cdot \boldsymbol{f}_{0,0}/r' - 3r'\,\boldsymbol{f}_{0,0}) - 3\,\boldsymbol{f}_{0,0} + \hat{\boldsymbol{e}}_u\hat{\boldsymbol{e}}_u\cdot \boldsymbol{f}_{0,0}]. \tag{6.3}$$

The above equation illustrates the leading-order behaviour of the outer flow field when flow reversal occurs. When $\hat{\boldsymbol{e}}_u$ reverses its direction, the Stokesian force $\boldsymbol{f}_{0,0}$ also acts in the opposite direction. However, this does not imply the entire reversal of the leading-order correction field $\boldsymbol{u}^{(0)}_{0,2}$. When the body moves in the opposite direction, one part of this field, $\hat{\boldsymbol{e}}_u\cdot\nabla'(\boldsymbol{r}'\boldsymbol{r}'\cdot \boldsymbol{f}_{0,0}/r' - 3r'\,\boldsymbol{f}_{0,0})/32\pi$, remains unchanged whereas the remainder, $(-3\,\boldsymbol{f}_{0,0} + \hat{\boldsymbol{e}}_u\hat{\boldsymbol{e}}_u\cdot \boldsymbol{f}_{0,0})/32\pi$, switches its direction.

6.2. *Second-order intermediate solution*

The second-order intermediate solutions have slightly different forms for $n=0$ and $n\neq 0$. Therefore, we consider these two cases separately.

When $n=0$, the governing equation for $\tilde{\boldsymbol{u}}_{02}$ is derived from (2.10*b*) and solved along with the proper boundary conditions at infinity and at the origin given by (2.12):

$$\tilde{\boldsymbol{u}}_{0,2} = \frac{1}{32\pi}[\hat{\boldsymbol{e}}_u\cdot\tilde{\nabla}(\tilde{\boldsymbol{r}}\tilde{\boldsymbol{r}}/\tilde{r} - 3\tilde{r}\boldsymbol{I}) + (\hat{\boldsymbol{e}}_u\hat{\boldsymbol{e}}_u - 3\boldsymbol{I})]\cdot \boldsymbol{f}_{0,0} + \boldsymbol{T}(\tilde{\boldsymbol{r}})\cdot \boldsymbol{f}_{0,1} + \boldsymbol{S}(\tilde{\boldsymbol{r}}):\boldsymbol{g}_{0,0}. \tag{6.4}$$

From (6.4), we can conclude that,

$$\tilde{\boldsymbol{u}}^{(0)}_{0,2} = \boldsymbol{u}^{(0)}_{0,2} = \frac{1}{32\pi}[\hat{\boldsymbol{e}}_u\cdot\tilde{\nabla}(\tilde{\boldsymbol{r}}\tilde{\boldsymbol{r}}/\tilde{r} - 3\tilde{r}\boldsymbol{I}) + (\hat{\boldsymbol{e}}_u\hat{\boldsymbol{e}}_u - 3\boldsymbol{I})]\cdot \boldsymbol{f}_{0,0}. \tag{6.5}$$

which we use to derive the matching condition for the inner region. The similarity between (6.3) and (6.5) appears to be due to the absence of the unsteady term in the intermediate equation for $n=0$.

When $n\neq 0$, we obtain $\tilde{\boldsymbol{u}}_{n,2}$ by solving the relevant equations in a similar fashion:

$$\tilde{\boldsymbol{u}}_{n,2} = -\hat{\boldsymbol{e}}_u\cdot\tilde{\nabla}\tilde{\boldsymbol{T}}_{n2}(\tilde{\boldsymbol{r}})\cdot \boldsymbol{f}_{n,0} + \tilde{\boldsymbol{T}}_n(\tilde{\boldsymbol{r}})\cdot \boldsymbol{f}_{n,1} + \boldsymbol{g}_{n,0}:\tilde{\nabla}\tilde{\boldsymbol{T}}_n(\tilde{\boldsymbol{r}}). \tag{6.6}$$

Here, the first term on the right-hand side of (6.6) is the particular integral for the governing equation and the other terms are general solutions to satisfy the boundary conditions. The second-order tensor $\tilde{\boldsymbol{T}}_{n2}$ is

$$\tilde{\boldsymbol{T}}_{n2}(\tilde{\boldsymbol{r}}) = \frac{1}{8\pi\tilde{r}}\left[\boldsymbol{I}\,\alpha_n(\tilde{r}) + \frac{\tilde{\boldsymbol{r}}\tilde{\boldsymbol{r}}}{\tilde{r}^2}\,\beta_n(\tilde{r})\right], \tag{6.7}$$

where the scalar functions α_n and β_n are

$$\alpha_n(\tilde{r}) = \frac{1}{3n^2\,Sl^2\,\tilde{r}^2}\left[3\mathrm{e}^{-c_n\tilde{r}}\left(c_n^3\tilde{r}^3 + c_n^2\tilde{r}^2 + 2c_n\tilde{r} + 2\right) - 2\left(c_n^3\tilde{r}^3 + 3\right)\right] \quad (n\neq 0), \tag{6.8}$$

$$\beta_n(\tilde{r}) = \frac{1}{n^2\,Sl^2\,\tilde{r}^2}\left[6 - \mathrm{e}^{-c_n\tilde{r}}\left(c_n^3\tilde{r}^3 + 3c_n^2\tilde{r}^2 + 6c_n\tilde{r} + 6\right)\right] \quad (n\neq 0). \tag{6.9}$$

We also determine $\tilde{\boldsymbol{u}}^0_{n2}$ which is necessary for the derivation of $\boldsymbol{u}_{n2}$:

$$\tilde{\boldsymbol{u}}^0_{n2} = -\frac{c_n}{6\pi}\,\boldsymbol{f}_{n,1} + \frac{1}{32\pi}(\mathrm{i}n\,Sl\,\boldsymbol{g}_{n,0} - \boldsymbol{f}_{n,0}\,\hat{\boldsymbol{e}}_u):\tilde{\nabla}(3\tilde{r}\boldsymbol{I} - \tilde{\boldsymbol{r}}\tilde{\boldsymbol{r}}/\tilde{r}). \tag{6.10}$$

For $|n|=3$, in general, $\boldsymbol{g}_{\pm 3,0}$ are non-zero. Therefore, though, for $|n|>2$, both $\boldsymbol{f}_{n,0}$ and $\boldsymbol{f}_{n,1}$ are zero, there is still a non-zero contribution to $\tilde{\boldsymbol{u}}^0_{n2}$ when $n=\pm 3$.

6.3. *Second-order inner solution*

The second-order inner equation is obtained from (2.6*b*) in the form

$$\nabla^2 \boldsymbol{u}_{n,2} - \nabla p_{n,2} = \mathrm{i}\, n\, Sl\, \boldsymbol{u}_{n,0} + \sum_{j=-\infty}^{\infty} \boldsymbol{u}_{j,0} \cdot \nabla \boldsymbol{u}_{n-j,0} = \boldsymbol{s}_n, \tag{6.11}$$

where the source term on the right-hand side of (6.11) is defined as $\boldsymbol{s}_n$. For an arbitrary body, zeroth-order inner fields $\boldsymbol{u}_{n,0}$ are not explicitly described in (3.4) where they are expressed in terms of $\boldsymbol{K}^{\mathrm{i}}_u$ and $\boldsymbol{K}^{\mathrm{i}}_\Omega$ without presenting functional forms of these tensors. Therefore, the analytical expression for $\boldsymbol{s}_n$ is not known and the close form explicit solution for $\boldsymbol{u}_{n,2}$ is impossible to derive. However, the second-order force can still be determined from (6.11) in an integral form (Brenner & Cox 1963; Lovalenti & Brady 1993).

In order to deduce the integral expression, we take the inner product of (6.11) with $\boldsymbol{K}_u$ and integrate it over the entire volume, excluding the space occupied by the particle. To simplify the integral, we use integration by parts and the divergence theorem while considering $\boldsymbol{u}_{n,2}=0$ at the body surface ($\mathscr{B}$) and

$$\boldsymbol{K}_u|_{\mathscr{B}} = \boldsymbol{I}, \qquad \nabla \cdot \boldsymbol{K}_u = 0, \qquad \nabla^2 \boldsymbol{K}_u = \nabla \boldsymbol{k}_u, \tag{6.12}$$

where $\boldsymbol{k}_u$ is a vector. After simplifying the integral equation, the second-order correction of the hydrodynamic force $\boldsymbol{f}_2$ is obtained

$$\frac{\boldsymbol{f}_2}{\eta U L\, Re} = \sum_{n=-\infty}^{\infty} \mathrm{e}^{\mathrm{i}nt} \int_{\mathscr{B}} \hat{\boldsymbol{n}}_{\mathscr{B}} \cdot (\nabla \boldsymbol{u}_{n,2} - p_{n,2}\boldsymbol{I})\, \mathrm{d}S = \sum_{n=-\infty}^{\infty} \mathrm{e}^{\mathrm{i}nt} \left(\int_{\Gamma} \bar{\boldsymbol{a}}_n\, \mathrm{d}S - \int_{\Gamma\mathscr{B}} \bar{\boldsymbol{b}}_n\, \mathrm{d}V \right), \tag{6.13}$$

where $\hat{\boldsymbol{n}}_{\mathscr{B}}$ is the unit outer normal vector on the body, Γ denotes the surface of an infinitely large sphere centred at the origin, $\Gamma\mathscr{B}$ is the entire external volume bounded by the surface of the infinite sphere and the outer surface of the particle, and, $\mathrm{d}S$ and $\mathrm{d}V$ are, respectively, the infinitesimal surface and volume element. The vectors $\bar{\boldsymbol{a}}_n$ and $\bar{\boldsymbol{b}}_n$ are

$$\bar{\boldsymbol{a}}_n = \hat{\boldsymbol{n}}_\Gamma \cdot (\nabla \boldsymbol{u}_{n,2} \cdot \boldsymbol{K}_u - p_{n,2}\boldsymbol{K}_u - \nabla \boldsymbol{K}_u \cdot \boldsymbol{u}_{n,2} + \boldsymbol{u}_{n,2}\boldsymbol{k}_u)|_{\boldsymbol{r}\to\infty}, \tag{6.14}$$

$$\bar{\boldsymbol{b}}_n = \boldsymbol{s}_n \cdot \boldsymbol{K}_u = \left(\mathrm{i}\, n\, Sl\, \boldsymbol{u}_{n,0} + \textstyle\sum \boldsymbol{u}_{j,0} \cdot \nabla \boldsymbol{u}_{n-j,0}\right) \cdot \boldsymbol{K}_u, \tag{6.15}$$

where $\hat{\boldsymbol{n}}_\Gamma$ is the unit outer normal vector on Γ. Considering the condition for $\boldsymbol{u}_{n,2}$ at infinity,

$$\boldsymbol{u}_{n,2}|_{\boldsymbol{r}\to\infty} = \tilde{\boldsymbol{u}}^{(0)}_{n,2}(\tilde{\boldsymbol{r}}) + \tilde{\boldsymbol{u}}^{(1)}_{n,1}(\tilde{\boldsymbol{r}}) Re^{-1/2}, \tag{6.16}$$

the right-hand side of (6.15) is evaluated using (6.10) and (4.8).

To derive $\boldsymbol{f}_{n2}$ in further detail, the vector integrands $\bar{\boldsymbol{a}}_n$ and $\bar{\boldsymbol{b}}_n$ are decomposed

$$\bar{\boldsymbol{a}}_n = \sum_{i=1}^{\infty} \bar{\boldsymbol{a}}^{(i)}_n, \qquad \bar{\boldsymbol{b}}_n = \sum_{i=2}^{\infty} \bar{\boldsymbol{b}}^{(i)}_n, \tag{6.17}$$

where $\bar{\boldsymbol{a}}^{(i)}_n$ and $\bar{\boldsymbol{b}}^{(i)}_n$ are terms which decay as r^{-i} with r. Among them, terms $\bar{\boldsymbol{a}}^{(i)}_n$ for $i>2$ do not contribute in the integral. The surface integral of $\bar{\boldsymbol{a}}^{(2)}_n$ at Γ and the volume integrals of terms $\bar{\boldsymbol{b}}^{(i)}_n$ in $\Gamma\mathscr{B}$ for $i>2$ are finite whereas the integrals involving $\bar{\boldsymbol{a}}^{(1)}_n$ and $\bar{\boldsymbol{b}}^{(2)}_n$ are individually infinite. However, a closer scrutiny of these terms shows

that the difference between these two infinite integrals is finite.

$$\int_{\Gamma} \bar{\boldsymbol{a}}_n^{(1)}\,\mathrm{d}S - \int_{\Gamma\mathscr{B}} \bar{\boldsymbol{b}}_n^{(2)}\,\mathrm{d}V = \int_{\mathscr{B}} \boldsymbol{c}_n\,\mathrm{d}S, \tag{6.18}$$

where

$$\boldsymbol{c}_n = \hat{\boldsymbol{n}}_{\mathscr{B}} \cdot \left(\nabla \boldsymbol{v}_{n,1}^{(1)} \cdot \boldsymbol{K}_{u(-1)} - \nabla \boldsymbol{K}_{u(-1)} \cdot \boldsymbol{v}_{n,1}^{(1)} + \boldsymbol{v}_{n,1}^{(1)} \boldsymbol{k}_{u(-1)}\right). \tag{6.19}$$

Here, $\boldsymbol{K}_{u(-i)}$ is given by $\boldsymbol{J}^T \cdot \boldsymbol{K}^{\mathrm{i}}_{u(-i)}(\boldsymbol{J}\cdot\boldsymbol{r})\cdot\boldsymbol{J}$ and $\boldsymbol{k}_{(-i)}$ is the corresponding vector defined in (6.12) with

$$\boldsymbol{v}_{n,1}^{(1)} = \sqrt{Re}\,\tilde{\boldsymbol{u}}_{n,1}^{(1)}(\tilde{\boldsymbol{r}}) = (\mathrm{i}\,n\,Sl/32\pi)(3r\boldsymbol{I} - \boldsymbol{r}\boldsymbol{r}/r)\cdot\boldsymbol{f}_{n0}. \tag{6.20}$$

The cancellation of two infinite integrals to produce a finite difference in (6.18) validates the expansions and matching conditions introduced in § 2.

Using (6.13)–(6.18), the second-order force can be expressed by non-zero finite integrals

$$\boldsymbol{f}_2 = \eta\, U\, L\, Re \sum_{n=-\infty}^{\infty} \mathrm{e}^{\mathrm{i}nt} \left(\int_{\Gamma} \boldsymbol{a}_n\,\mathrm{d}S - \int_{\Gamma\mathscr{B}} \boldsymbol{b}_n\,\mathrm{d}V + \int_{\mathscr{B}} \boldsymbol{c}_n\,\mathrm{d}S\right), \tag{6.21}$$

where the vector integrand $\boldsymbol{a}_n$ and $\boldsymbol{b}_n$ are such that they produce finite non-zero integrals

$$\boldsymbol{a}_n = \bar{\boldsymbol{a}}_n^{(2)}, \qquad \boldsymbol{b}_n = -\left[\mathrm{i}\,n\,Sl\,(\boldsymbol{u}_{n,0} - \boldsymbol{T}\cdot\boldsymbol{f}_{n,0}) + \textstyle\sum \boldsymbol{u}_{j,0}\cdot\nabla\boldsymbol{u}_{n-j,0}\right]\cdot\boldsymbol{K}_u. \tag{6.22}$$

In (3.13) and (4.15), we saw that the zeroth- and the first-order forces vibrate with only two frequencies. However, there are an infinite number of frequencies with which the second-order force vibrates because the integrands in (6.21) are in general non-zero for any n.

Rubinow & Keller (1961) derived the corrective force on a spinning sphere due to fluid inertia. This prior result can be obtained from (6.21) when a spherical body is considered to be rotating about its centre. In such a case, because of the spherical symmetry, only terms involving $n = 0$ are considered in (6.21) to recover the old result.

7. Conclusion

In this paper, the unsteady hydrodynamics of a steadily translating and rotating particle is analysed and the expression for the unsteady hydrodynamic force is derived. For this purpose, first we systematically describe the necessary Reynolds-number expansion to determine the effect of the unsteady flow field generated owing to the rotation of the particle. We take into account the periodicity of the fields with time and develop expansion equations and matching conditions accordingly.

Then we proceed to describe the leading-order solutions in our expansion. The key element in this derivation is the body invariance relation (3.5) which implies that the representation of relevant tensorial quantities in a set of basis vectors fixed with the body is time invariant. This relation is used to derive zeroth-order unsteady quantities.

Our analysis shows that the inherently unsteady leading-order flow field produces time-dependent Stokes resistance on the body. This force has a steady part and two other modes which vibrate with frequencies $1/2\pi$ and $1/\pi$. However, this unsteady phenomenon occurs only when the particle is rotating about an axis which is not its axis of rotational symmetry. When an axisymmetric body rotates around its axis of symmetry, we have shown that the vibrating modes of the hydrodynamic force vanish.

We systematically use the introduced Reynolds-number expansion to obtain the first-order inertial correction to the hydrodynamic force. Similar to the zeroth-order force, the first-order force also has a steady part and two vibrating modes with frequencies $1/2\pi$ and $1/\pi$ in (4.15). Because of the existence of the steady part, the time-averaged first-order force on the particle is non-zero. This suggests that the effect of the unsteady near-field correction due to the particle rotation not only has an instantaneous impact on the particle motion, but may also alter the long-time behaviour of the particle. However, it would be a matter of future work to establish this conjecture on a firm theoretical basis. Physically, the existence of a non-zero time-averaged first-order correction implies that, with respect to the real flow, the Stokes flow field has a preferential error which produces a finite force on the rotating–translating particle. The first-order force is proportional to $\sqrt{Re}$ and therefore, its effect on the particle is bigger than the effect of the Oseen correction.

We have applied our theoretical results to obtain the zeroth-order unsteady Stokesian force and the corresponding first-order inertial corrections for the clusters of rigidly connected spheres. Two types of cluster configuration are considered – linear chains of touching spheres and two-dimensional square arrays of attached spheres. Our results indicate that the line of action of the time-averaged first-order force and its temporal phase difference with the zeroth-order force are independent of the shape of the object considered if the angular velocity vector is along an eigenvector of the Stokes resistance tensor.

Finally, we also derive the integral expression for the second-order inertial correction to the hydrodynamic force in (6.21). The second-order force has an infinite number of vibrating modes. Though, for an arbitrary body, it is not possible to derive the exact analytical expression for this force, the finiteness of the integrals in the expression (6.21) validates the correctness of the analysis.

I would like to acknowledge the support provided by Jerzy Bławzdziewicz from the NSF grant CTS-0201131.

REFERENCES

Bhattacharya, S., Blawzdziewicz, J. & Wajnryb, E. 2005 Many-particle hydrodynamic interactions in parallel-wall geometry: Cartesian-representation method. *Physica* A **336**, 1–47.

Brenner, H. 1963 The Stokes resistance of an arbitrary particle. *Chem. Engng Sci.* **18**, 1–25.

Brenner, H. 1964 The Stokes resistance of an arbitrary particle – II An extension. *Chem. Engng Sci.* **19**, 599–629.

Brenner, H. & Cox, R. 1963 The resistance to a particle of arbitary shape in translational motion at small Reynolds number. *J. Fluid Mech.* **17**, 561–596.

Chester, W. 1990 A general theory for the motion of a body through a fluid at low Reynolds number. *Proc. R. Soc. Lond.* A **430**, 89–104.

Cox, R. 1965 The steady motion of a particle of arbitary shape at small Reynolds number. *J. Fluid Mech.* **23**, 625–643.

Gavze, E. 1990 The accelerated motion of a rigid body in non-steady Stokes flow. *Intl J. Multiphase Flow* **16**, 153–166.

Khayat, R. & Cox, R. 1989 Inertia effects on the motion of long slender bodies. *J. Fluid Mech.* **209**, 435.

Lawrence, C. & Weinbaum, S. 1986 The force on an axisymmetric body in linearized time dependent motion. *J. Fluid Mech.* **171**, 209–218.

Lawrence, C. & Weinbaum, S. 1988 Unsteady force on a body at low Reynolds number. *J. Fluid Mech.* **189**, 463–489.

Leshansky, A., Lavrenteva, O. & Nir, A. 2004 The leading effect of fluid inertia on the motion of rigid bodies at low Reynolds number. *J. Fluid Mech.* **505**, 235–248.

Lovalenti, P. & Brady, J. 1993 The hydrodynamic force on a rigid particle undergoing arbitary time dependent motion at small Reynolds number. *J. Fluid Mech.* **256**, 561–605.

Lovalenti, P. & Brady, J. 1995 The temporal behaviour of the hydrodynamic force on a body in response to an abrupt change in velocity at small Reynolds number. *J. Fluid Mech.* **293**, 35–46.

Maxey, M. & Riley, J. 1983 Equation of motion for a small rigid sphere in non-uniform flow. *Phys. Fluids* **26**, 883–889.

Mazur, P. & Bedeaux, D. 1974 A generalization of Faxén's theorem to nonsteady motion of a sphere through an incompressible fluid in arbitrary flow. *Physica* **76**, 235–46.

Mei, R., Lawrence, C. & Adrian, R. 1992 Unsteady drag on a sphere at finite Reynolds number with small fluctuation in free-stream velocity. *J. Fluid Mech.* **233**, 613–631.

Pittman, J. & Kasiri, N. 1992 The motion of rigid rod-like particles suspended in non-homogeneous flow-field. *Intl J. Multiphase Flow* **18**, 1077–1091.

Rubinow, S. & Keller, J. 1961 The transverse force on a spinning sphere moving in a viscous fluid. *J. Fluid Mech.* **15**, 447–459.

Saffman, P. 1965 The lift on a small sphere in a slow shear flow. *J. Fluid Mech.* **22**, 385–400 and Corrigendum (1968) **31**, 624.

Youngren, G. & Acrivos, A. 1975 Stokes flow past a particle of arbitary shape: a numerical method of solution. *J. Fluid Mech.* **69**, 377–403.